

**Measurement of the neutrino-oxygen
neutral-current quasielastic cross section using
atmospheric neutrinos in the SK-Gd experiment**

Graduate School of Natural Science and Technology
Okayama University

Seiya Sakai

March 1, 2024

ABSTRACT

Neutrino is neutrino.
Do you know neutrino?

ACKNOWLEDGMENTS

Thank you so much!

Contents

1	Neutrino	1
1.1	What is neutrino?	1
2	Super-Kamiokande	2
2.1	Super-Kamiokande	2
2.2	ID PMT	3
2.3	OD PMT	6
2.4	Helmholtz coils	6
2.5	Observation phase	7
2.6	Detection principle	9
A	Neutrino	11
A.1	What is neutrino?	11

List of Figures

2.1	Overview of the Super-Kamiokande detector	2
2.2	Cross section of the SK detector and overview of supermodule frames	3
2.3	Schematic view of the ID PMT	4
2.4	Quantum efficiency of the ID PMT photocathode as a function of wavelength	4
2.5	Single photoelectron pulse height distribution of the ID PMT	5
2.6	Relative transit time distribution for a typical ID PMT tested using 410 nm wavelength light at the single photoelectron intensity level	5
2.7	Positional relationship of ID PMTs and OD PMTs in a supermodule frame	6
2.8	Schematic view of Helmholtz coils	7
2.9	Picture of a shockwave prevention case	8
2.10	Schematic view of Cherenkov radiation	10

List of Tables

2.1	Information of each observation phase	9
2.2	Cherenkov threshold of main charged particles	10

1 Neutrino

1.1 What is neutrino?

Neutrino is neutrino.
Do you know neutrino?

2 Super-Kamiokande

2.1 Super-Kamiokande

The Super-Kamiokande (SK) [1] is the experiment held in Kamioka, Gifu, Japan, with the large water Cherenkov detector placed in 1,000 m underground, 2,700 m water equivalent overburden. The overview of the SK detector is shown in Figure 2.1. The SK stands for “Super-Kamioka Neutrino Detection Experiment” and “Super-Kamioka Nucleon Decay Experiment”. The rate of cosmic ray muon is reduced by a factor of 10^5 compared to that of the ground level.

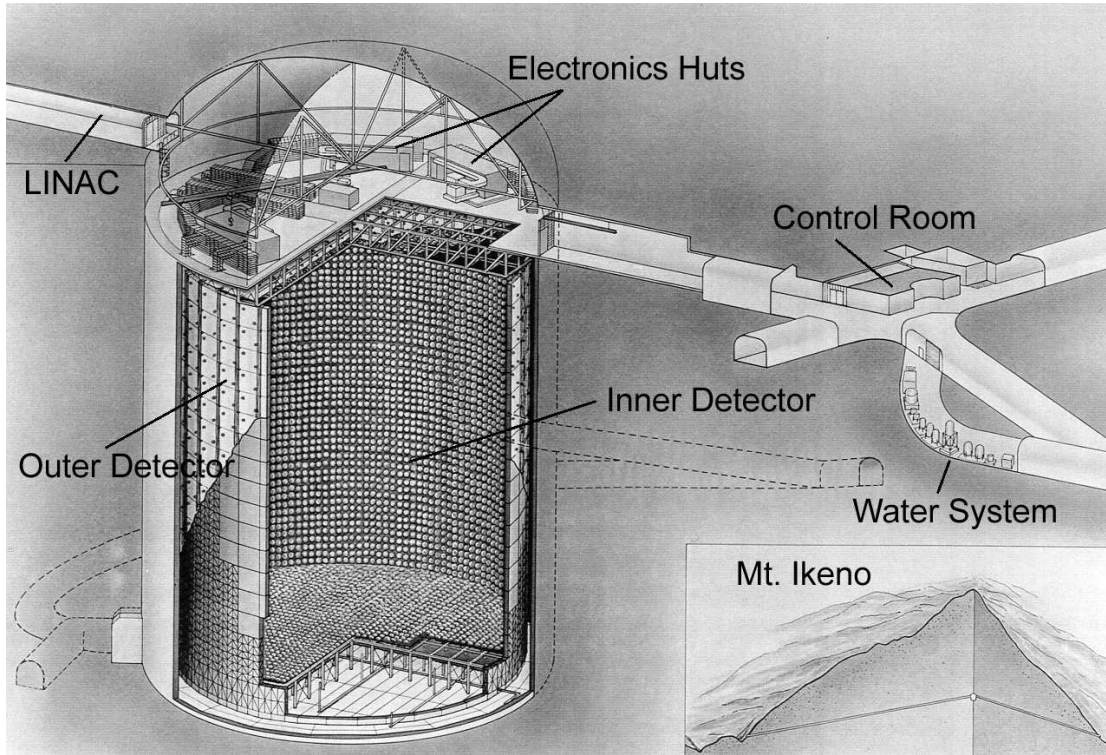


Figure 2.1: Overview of the SK detector [1].

The SK detector consists of the stainless-steel cylindrical tank with a diameter of 39.3 m and a height of 41.4 m and 50 kilotons ultrapure water. The tank is separated into the inner detector (ID) and the outer detector (OD) by stainless-steel frames (supermodule frames). The cross section of the SK detector and the overview of supermodule frames are shown in Figure 2.2. The diameter of ID, the height of ID and the volume of ID (the fiducial volume) is 33.8 m, 36.2 m and 32 kilotons (22.5 kilotons), respectively. In ID, 11,129 20-inch (50 cm) photomultiplier tubes (PMTs) are installed. The gaps between ID PMTs are covered by black polyethylene terephthalate sheets. The

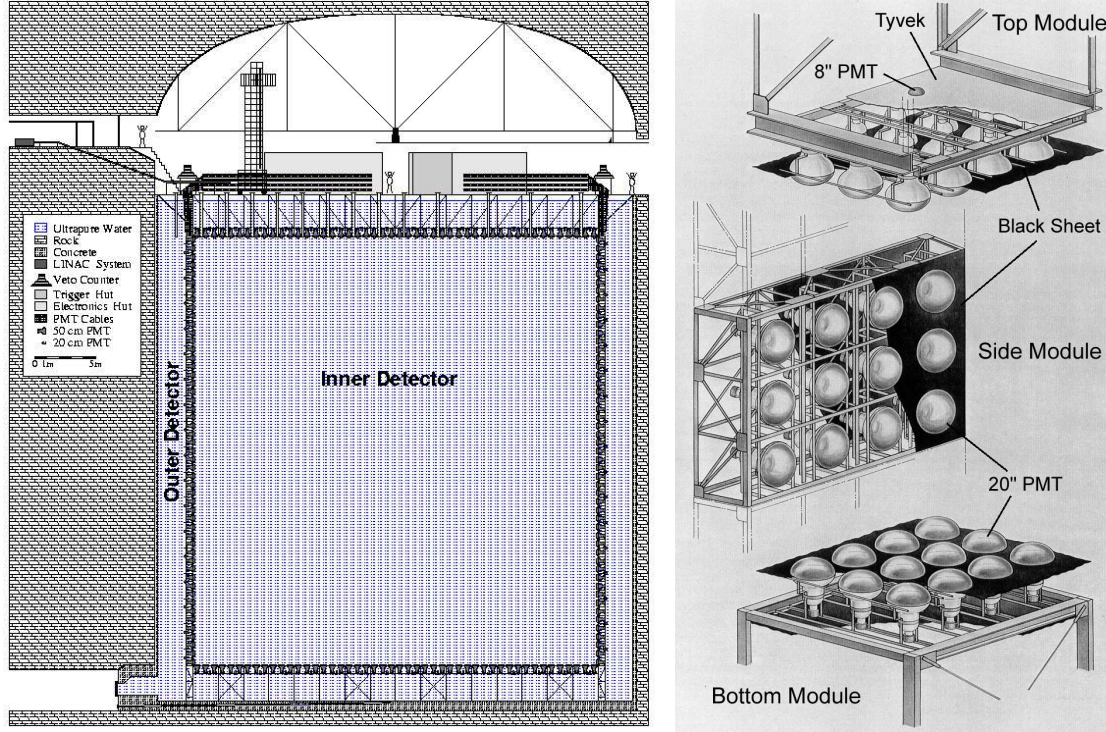


Figure 2.2: Cross section of the SK detector (left) and overview of supermodule frames (right) [1].

sheets separate ID and OD optically and suppress the reflection at the surface of the ID wall. Moreover, the sheets reduce low energy events by radioactive backgrounds occurring behind the PMTs. On the other hand, in OD, 1,885 8-inch (20 cm) PMTs are installed. OD volume is covered by white Tyvek sheets manufactured by DuPont. The Tyvek sheets have high reflectivity and enhance the light collection efficiency in OD.

2.2 ID PMT

The schematic view of the ID PMT is shown in Figure 2.3. The number of ID PMTs is 7,650 on the barrel (side walls), 1,740 on the top and 1,739 on the bottom, thus the effective photocathode coverage of ID is 40%. The role of ID PMTs is to reconstruct the energy, generated position, direction and the kind of the charged particles. Figure 2.4 shows the quantum efficiency of the ID PMT photocathode as a function of wavelength. The material of photocathode is bialkali (Sb-K-Cs) and the quantum efficiency is about 21% at 360 - 400 nm. Figure 2.5 shows the single photoelectron pulse height distribution of the ID PMT. The peak around zero ADC count is caused by PMT dark current. Figure 2.6 shows the relative transit time distribution for a typical ID PMT tested using 410 nm wavelength light at the single photoelectron intensity level. The 1σ of transit time for a single photoelectron signal is 2.16 ns.

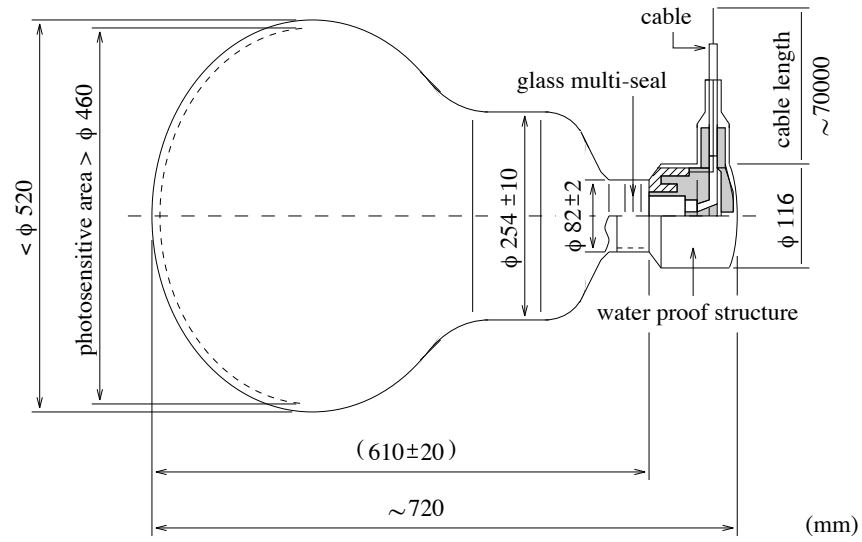


Figure 2.3: Schematic view of the ID PMT [1].

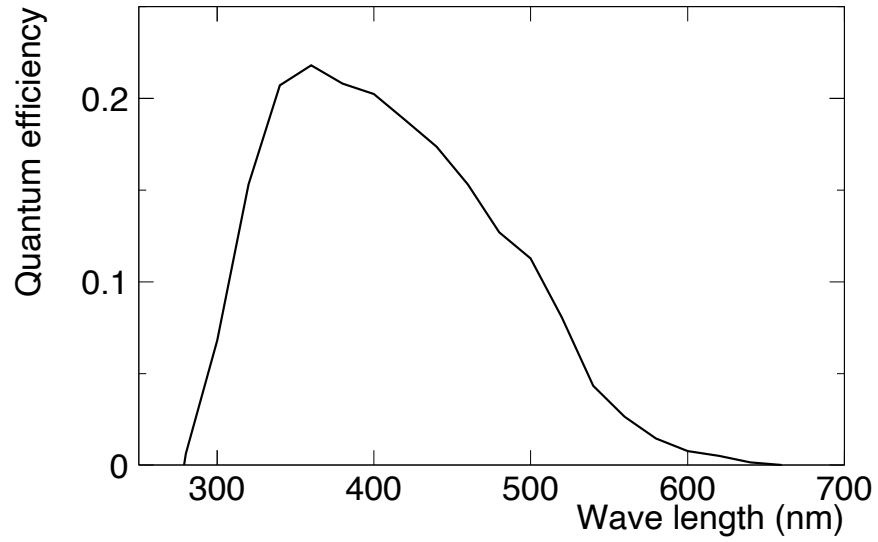


Figure 2.4: Quantum efficiency of the ID PMT photocathode as a function of wavelength [1]. The material of ID PMT photocathode is bialkali (Sb-K-Cs).

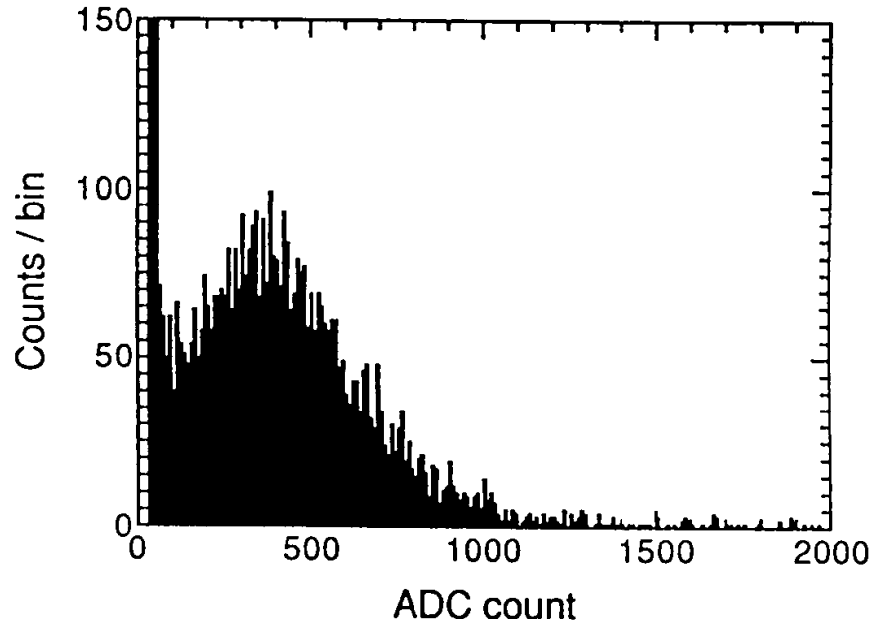


Figure 2.5: Single photoelectron pulse height distribution of the ID PMT [1]. The peak around zero ADC count is caused by PMT dark current.

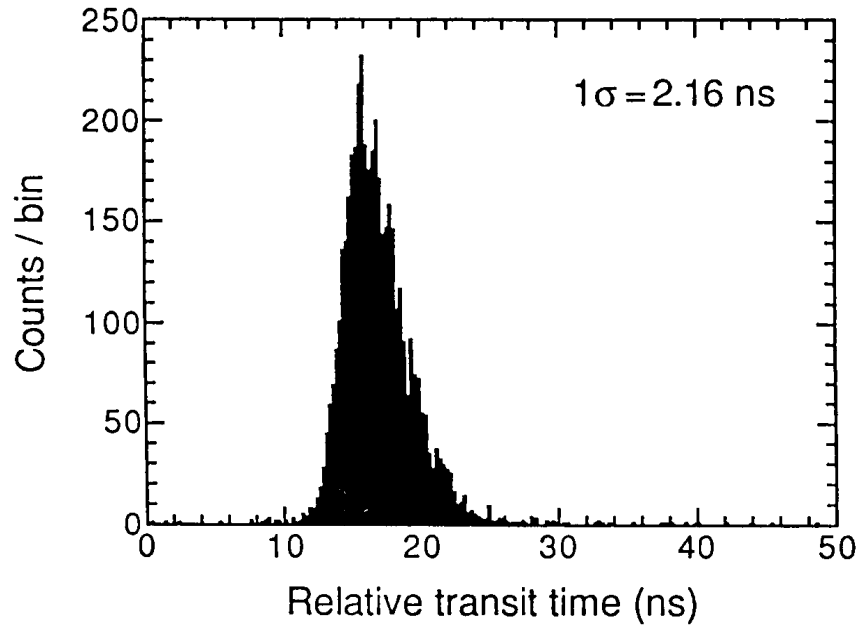


Figure 2.6: Relative transit time distribution for a typical ID PMT tested using 410 nm wavelength light at the single photoelectron intensity level [1].

2.3 OD PMT

The number of OD PMTs is 1,275 on the barrel, 302 on the top and 308 on the bottom. To compensate the small number of OD PMTs, wavelength shifting (WS) plate is attached to each OD PMT. The WS plate is square acrylic panel with a side of 60 cm and a thickness of 1.3 cm, doped with 50 mg/L of bis-MSB ($C_{24}H_{22}$). The WS plate absorbs UV light, and then emit photons in the blue - green. OD PMT with bialkali photocathode is more sensitive to blue - green photons than UV photons. Therefore, the light collection efficiency is improved by about a factor of 1.5 compared to without WS plates. The timing resolution of OD PMTs with WS plates is 15 ns (FWHM), which is poorer than that of ID PMTs. However, OD was optimized as a veto counter and the poorer timing resolution is less important. Figure 2.7 shows the positional relationship of ID PMTs and OD PMTs in a supermodule frame. Basically, in a supermodule frame, 12 ID PMTs and 2 OD PMTs are attached.

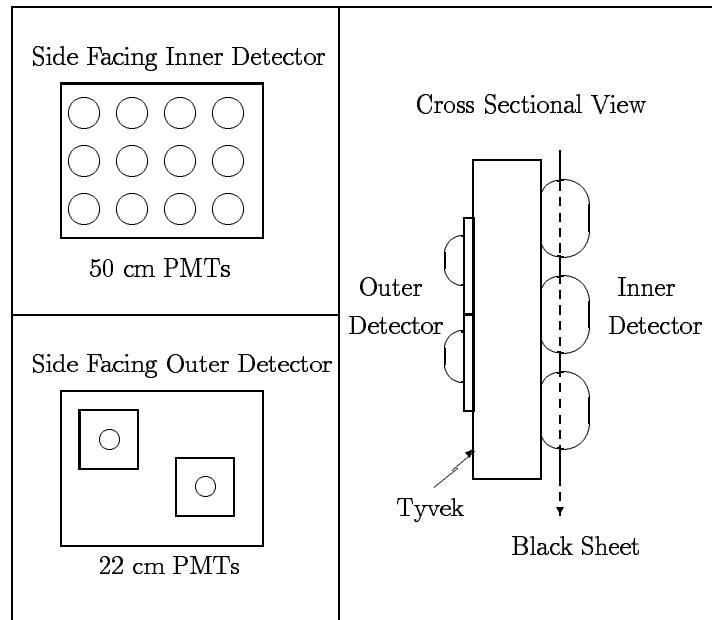


Figure 2.7: Positional relationship of ID PMTs and OD PMTs in a supermodule frame [2]. 12 ID PMTs and 2 OD PMTs are attached in a supermodule frame, basically.

2.4 Helmholtz coils

The geomagnetic field would affect photoelectron trajectories and timing in the PMTs. Therefore, 26 sets of horizontal and vertical Helmholtz coils are deployed around the inner surface of the tank to reduce the geomagnetic field. Figure 2.8 shows the schematic view of Helmholtz coils. The

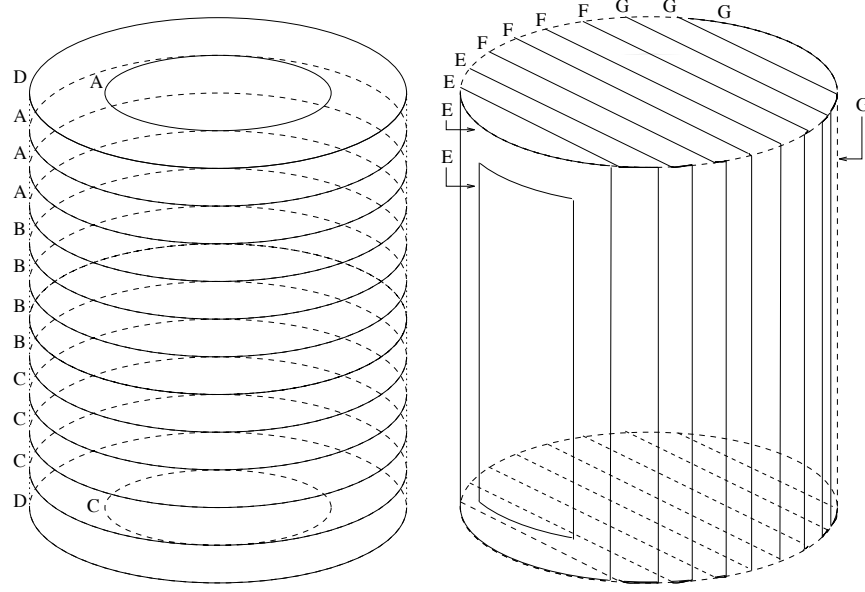


Figure 2.8: Schematic view of Helmholtz coils [4].

average geomagnetic field intensity without Helmholtz coils is about 450 mG [1]. The average field intensity can be reduced to 32 mG with Helmholtz coils, resulting that the deviation in the collection efficiency of photoelectrons is 2% [3].

2.5 Observation phase

The observation phase of SK is categorized into seven, from SK-I to SK-VII. Each observation phase is described below.

SK-I

SK-I started in April 1996 and ended in July 2001. In ID, 11,146 PMTs were attached and the effective photocathode coverage of ID was 40%. It was during the SK-I that we got the evidence for neutrino oscillation [5].

SK-II

In November 12th, 2001, one bottom PMT broke when ultrapure water was filled into SK detector after finishing the detector maintenance. Due to the shockwave generated at that time, other PMTs were broken in a chain. As a result, it became a serious accident that 6,779 ID PMTs and 1,017 OD PMTs were lost. In SK-II, which started in October 2002 and ended in October 2005, the observation was performed using 5,182 remained and spare ID PMTs and 1,885 remained and new OD PMTs. The effective photocathode coverage of ID was 19%. Since SK-II, each ID PMT



Figure 2.9: Picture of a shockwave prevention case [6].

has been covered with a shockwave prevention case. The case consists of an acrylic that covers the photocathode and Fiber Reinforced Plastic (FRP) case that covers parts other than the photocathode. The case not only prevents shockwave but also increases the water pressure resistance of the PMT. The picture of a shockwave prevention case is shown in Figure 2.9.

SK-III

SK-III started in July 2006 and ended in August 2008. Since SK-III, the number of ID PMTs has been 11,129 and the effective photocathode coverage of ID has been 40%. The reason why the number of ID PMTs is reduced by 17 compared to SK-I is that ID PMTs cannot be installed at the edge of the detector because the size of the shockwave prevention case is large.

SK-IV

In September 2008, the data acquisition system was renewed from Analog Timing Module (ATM) to QTC-Based Electronics with Ethernet (QBEE) and SK-IV started [7]. QTC stands for charge-to-time converter. The renewal of the system allows us to open the data acquisition time window until $535 \mu\text{s}$ from the trigger timing and enabled to search neutron signals [8]. SK-IV continued until June 2018 and is longest phase at this time.

SK-V

The tank refurbishment work toward the SK-Gd experiment was conducted between SK-IV and SK-V. The purpose of the work was the water stop reinforcement of the tank, the piping improvement in the tank and the PMT replacement. After finishing the work, SK-V started in January 2019 and ended in July 2020.

SK-VI

In July 2020, we dissolved 13.2 tons of $\text{Gd}_2(\text{SO}_4)_3 \cdot 8\text{H}_2\text{O}$ (we introduced 0.011% of Gd) into the

SK tank and SK-VI (the SK-Gd experiment) started. The time constant of neutron capture at this Gd concentration is about $115 \mu\text{s}$ [9]. SK-VI continued until June 2022.

SK-VII

In June 2022, we additionally dissolved 27.3 tons of $\text{Gd}_2(\text{SO}_4)_3 \cdot 8\text{H}_2\text{O}$ into the SK tank and SK-VII started. The Gd concentration is comparable to 0.03%. The time constant of neutron capture at this Gd concentration is about $62 \mu\text{s}$.

The information of each observation phase is summarized in Table 2.1.

Table 2.1: Information of each observation phase.

Phase	SK-I	SK-II	SK-III
Start	Apr. 1996	Oct. 2002	Jul. 2006
End	Jul. 2001	Oct. 2005	Sep. 2008
# of ID PMTs (Coverage)	11,146 (40%)	5,182 (19%)	11,129 (40%)
# of OD PMTs	1,885	1,885	1,885
Electronics	ATM	ATM	ATM
Gd concentration	0%	0%	0%

Phase	SK-IV	SK-V	SK-VI	SK-VII
Start	Sep. 2008	Jan. 2019	Jul. 2020	Jun. 2022
End	Jun. 2018	Jul. 2020	Jun. 2022	-
# of ID PMTs (Coverage)	11,129 (40%)	11,129 (40%)	11,129 (40%)	11,129 (40%)
# of OD PMTs	1,885	1,885	1,885	1,885
Electronics	QBEE	QBEE	QBEE	QBEE
Gd concentration	0%	0%	0.011%	0.03%

2.6 Detection principle

When the speed of the charged particle passing through the dielectric medium is faster than the speed of light in the medium, photons are radiated conically along the track of the particle. This phenomenon is called “Cherenkov radiation”, and the radiated photons are called “Cherenkov photons”. Figure 2.10 shows the schematic view of Cherenkov radiation. In Figure 2.10, the charged particle with velocity v moves distance $vt = \frac{v}{c}ct = \beta ct$ in time t , where c is the speed of light in vacuum and $\beta = \frac{v}{c}$ is the ratio of v and c . While the Cherenkov photon moves distance $\frac{c}{n}t$ in time t , where n is the refractive index of the dielectric medium. Therefore, when the angle between the direction of charged particle and the direction of Cherenkov photon is defined as θ_C ,

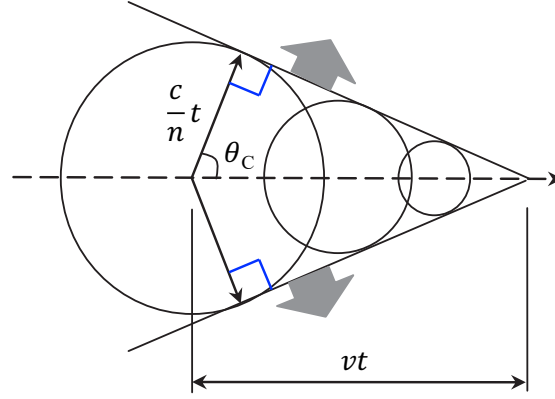


Figure 2.10: Schematic view of Cherenkov radiation [10].

the next formula is established,

$$\cos \theta_C = \frac{\frac{c}{n}t}{\beta ct} = \frac{1}{n\beta}. \quad (2.1)$$

In Equation (2.1), assuming that $n = 1.34$, which is the refractive index of water, and $\beta = 1$, θ_C becomes about 42° . Therefore, in water, the maximum angle between the direction of charged particle and the direction of Cherenkov angle is about 42° .

The energy E required for the charged particle with rest mass m to emit Cherenkov photons (Cherenkov threshold) is

$$E = \frac{mc^2}{\sqrt{1 - \beta^2}} \geq \frac{mc^2}{\sqrt{1 - \left(\frac{1}{n}\right)^2}} = \frac{nmc^2}{\sqrt{n^2 - 1}}. \quad (2.2)$$

The Cherenkov threshold of main charged particles is summarized in Table 2.2.

Table 2.2: Cherenkov threshold of main charged particles [11]. m is rest mass and E is Cherenkov threshold. Here $n = 1.34$ is assumed.

Charged particle	e^\pm	μ^\pm	π^\pm	K^\pm	p
m [MeV/ c^2]	0.511	105.658	139.570	493.677	938.272
E [MeV]	0.768	158.730	209.676	741.652	1,409.568

A Neutrino

A.1 What is neutrino?

Neutrino is neutrino.
Do you know neutrino?

References

- [1] S. Fukuda *et al.*, Nucl. Instrum. Methods Phys. Res., Sect. A **501**, 418 (2003).
- [2] Z. Conner, “A STUDY OF SOLAR NEUTRINOS USING THE SUPER-KAMIOKANDE DETECTOR”, Ph.D. Thesis, University of Maryland (1997).
- [3] K. Abe *et al.*, Nucl. Instrum. Methods Phys. Res., Sect. A **737**, 253 (2014).
- [4] T. Yamaguchi, “Observation of ^8B Solar Neutrinos from 300-day data at Super-Kamiokande”, Ph.D. Thesis, University of Osaka (1998).
- [5] Y. Fukuda *et al.*, Phys. Rev. Lett. **81**, 1562–1567 (1998).
- [6] “Report from cause committee”, <https://www-sk.icrr.u-tokyo.ac.jp/cause-committee/> (2003).
- [7] H. Nishino *et al.*, Nucl. Instrum. Methods Phys. Res., Sect. A **610**, 710 (2009).
- [8] H. Watanabe *et al.*, Astropart. Phys. **31**, 320 (2009).
- [9] K. Abe *et al.*, Nucl. Instrum. Methods Phys. Res., Sect. A **1027**, 166248 (2022).
- [10] K. Yamamoto *et al.*, “Application of Cherenkov Light Observation to Reactor Measurements (1) - Estimation of Reactor Power from Cherenkov Light Intensity -”, JAEA-Technology 2014-028 (2015).
- [11] R. L. Workman *et al.*, Prog. Theor. Exp. Phys. **2022**, 083C01 (2022).